Paleoclimatological perspective on river basin hydrometeorology: case of the Mekong Basin

Räsänen, T.A.; Lehr, C.; Mellin, I.; Ward, P.J.; Kummu, M.S.

published in
Hydrology and Earth System Sciences
2013

DOI (link to publisher)
10.5194/hess-17-2069-2013

document version
Publisher's PDF, also known as Version of record

Hydrol. Earth Syst. Sci., 17, 2069–2081, 2013
www.hydrol-earth-syst-sci.net/17/2069/2013/
doi:10.5194/hess-17-2069-2013

Hydrology and Earth System Sciences
Open Access

Palaeoclimatological perspective on river basin hydrometeorology: case of the Mekong Basin

T. A. Räsänen[1], C. Lehr[1], I. Mellin[2], P. J. Ward[3,4], and M. Kummu[1]

[1]Water & Development Research Group, Department of Civil and Environmental Engineering, Aalto University, Espoo, Finland
[2]Department of Mathematics and Systems Analysis, Aalto University, Espoo, Finland
[3]Institute for Environmental Studies, VU University Amsterdam, Amsterdam, the Netherlands
[4]Amsterdam Global Change Institute, VU University Amsterdam, Amsterdam, the Netherlands

Correspondence to: T. A. Räsänen (timo.rasanen@aalto.fi)

Received: 15 October 2012 – Published in Hydrol. Earth Syst. Sci. Discuss.: 9 November 2012
Revised: 8 March 2013 – Accepted: 27 April 2013 – Published: 31 May 2013

Abstract. Globally, there have been many extreme weather events in recent decades. A challenge has been to determine whether these extreme weather events have increased in number and intensity compared to the past. This challenge is made more difficult due to the lack of long-term instrumental data, particularly in terms of river discharge, in many regions including Southeast Asia. Thus our main aim in this paper is to develop a river basin scale approach for assessing interannual hydrometeorological and discharge variability on long, palaeological, time scales. For the development of the basin-wide approach, we used the Mekong River basin as a case study area, although the approach is also intended to be applicable to other basins. Firstly, we derived a basin-wide Palmer Drought Severity Index (PDSI) from the Monsoon Asia Drought Atlas (MADA). Secondly, we compared the basin-wide PDSI with measured discharge to validate our approach. Thirdly, we used basin-wide PDSI to analyse the hydrometeorology and discharge of the case study area over the study period of 1300–2005. For the discharge-MADA comparison and hydrometeorological analyses, we used methods such as linear correlations, smoothing, moving window variances, Levene type tests for variances, and wavelet analyses. We found that the developed basin-wide approach based on MADA can be used for assessing long-term average conditions and interannual variability for river basin hydrometeorology and discharge. It provides a tool for studying interannual discharge variability on a palaeological time scale, and therefore the approach contributes to a better understanding of discharge variability during the most recent decades. Our case study revealed that the Mekong has experienced exceptional levels of interannual variability during the post-1950 period, which could not be observed in any other part of the study period. The increased variability was found to be at least partly associated with increased El Niño Southern Oscillation (ENSO) activity.

1 Introduction

Globally, the last decade has been a decade of extreme weather events, with record breaking events being observed in many regions of the world (Coumou and Rahmstorf, 2012). The Intergovernmental Panel on Climate Change (IPCC) reports that globally there is evidence that the number of weather and climate extremes, of warm spells or heat waves and heavy precipitation, has increased since 1950, but that large regional differences exist (IPCC, 2012). Many of these changes have been linked to anthropogenic global warming but also to natural climate variability (IPCC, 2012). Due to the limited availability of long-term observed records of climatological and hydrological parameters, a major challenge has been determining whether the frequency or intensity of extreme events have increased (IPCC, 2012). To overcome this deficiency, data periods have been extended by reconstructing past climates with palaeoclimate proxies (e.g. Dobrovolny et al., 2010; Cook et al., 2007).

In terms of floods, there is limited evidence of climate driven changes in the magnitudes and frequencies at regional

Published by Copernicus Publications on behalf of the European Geosciences Union.

and global scales (IPCC, 2012). Some palaeohydrological modelling efforts have been carried out to try to examine Holocene discharge changes compared to recent (and future) changes (e.g. Bogaart et al., 2003; Notebaert et al., 2011; Renssen et al., 2007; Ward et al., 2008, 2011). Aerts et al. (2006), for example, simulated river discharge for 15 large river basins around the globe over the period 9000 BP to 2100 AD, and found that for many of the basins the projected change in mean annual discharge during the 21st century is of similar magnitude, or larger, than the change during the last 9000 yr. However, these past studies only examine long-term changes in average flows, and do not specifically address variability. Also, little is known on how recent hydrological variation compares to hydrological variability on the palaeological time scale.

For monsoon regions, there remains considerable uncertainty with regards to the current understanding on climate change related extreme events (IPCC, 2012). However, the recently developed Monsoon Asia Drought Atlas (MADA) (Cook et al., 2010) may provide important information on monsoon variability at the centennial scale. The MADA is a Monsoon Asia-wide Palmer Drought Severity Index (PDSI) dataset describing summer monsoon conditions over the period 1300–2005. To date, the MADA has been applied and investigated in just a few studies (e.g. Bell et al., 2011; Anchukaitis et al., 2010; Fang et al., 2013; Ummenhofer et al., 2013), but none of these have used MADA on a river basin scale, linked it to discharge variability or examined in detail how well it can be used for the investigation of hydrometeorological variability induced by phenomena such as the El Niño Southern Oscillation (ENSO).

We believe that it is very important to understand the current hydroclimate and river discharge variability from a palaeological perspective in Monsoon Asia, as the region is home to more than half of the world's population, and a large part of their livelihoods, and moreover food security is based on local hydroclimatological conditions (see e.g. Wassmann et al., 2009). If the current variability can be put into a longer time perspective, we believe that it would help to understand the stresses of possible changes in hydroclimatic variability on aquatic ecosystems, traditional livelihoods and other societal functions.

In this paper our aim is thus to develop an approach for assessing the long-term variability of hydrometeorological conditions and river discharge in large river basins in Monsoon Asia. The approach can be used to increase the understanding of the most recent interannual hydrometeorology and discharge variability, and placing this is in a longer palaeological time scale. Thus, the approach aims to contribute to the filling of the research gap on the limited evidence with regards to discharge changes during recent decades (see IPCC, 2012). The approach we develop is based on the MADA dataset, and it has three main steps: (i) constructing a basin-wide PDSI from MADA; (ii) comparing the characteristics of the basin-wide PDSI with observed discharge in order to validate the approach; and (iii) analysing the variability of recent decades on a palaeological time scale of 700 yr. To achieve these steps successfully, we used various statistical and signal analysis methods.

We selected the Mekong River basin as a case study to test our approach, as the Mekong's climate is strongly influenced by the Asian monsoon (Delgado et al., 2012); the basin has experienced very wet and very dry years in recent decades (Te, 2007; MRC, 2010, 2011a, b); and there is good MADA and discharge data coverage in the basin. The annual flood pulse, as well as droughts, play a key role in the Mekong Basin, as the region's ecosystems, livelihoods, and economic activities are largely based on rainfed agriculture and aquatic ecosystems (MRC, 2010; Baran and Myschowoda, 2009; Chinvanno et al., 2008). It is thus important to understand the hydrometeorological and discharge variability in the basin.

2 Case study area and past research

2.1 The Mekong Basin

The Mekong River basin (Fig. 1) is the largest basin in Southeast Asia. It originates from the high elevations of the Tibetan Plateau and flows approximately 4800 km before discharging its waters into the South China Sea (MRC, 2005). The land area of the basin is 795 000 km^2, and is shared by China (21 % of total land area), Myanmar (3 %), Thailand (23 %), Lao PDR (25 %), Cambodia (20 %) and Vietnam (8 %) (MRC, 2005).

The climate of the Mekong is characterised by wet and dry seasons generated by the southwest (May–October) and northeast monsoons (November–April) (MRC, 2005). The annual average rainfall of the Mekong Basin is approximately 1400 mm, ranging from 300 to 3000 mm between individual measurement stations (Räsänen and Kummu, 2013). The driest parts of the basin are located in the far north in the Tibetan Plateau and the wettest parts can be found in the east close to the Annamite mountain range (see locations in Fig. 1). The majority of the rainfall occurs during the months of the southwest monsoon, which leads to an annual hydrograph with a pulsing nature. Low flows are experienced in March–April (on average 1800 m^3 s^{-1} at Stung Treng; see location in Fig. 1) and high flows in August–September (on average 41 000 m^3 s^{-1} at Stung Treng) (Räsänen and Kummu, 2013). The annual average discharge of the Mekong is approximately 14 500 m^3 s^{-1}, or 475 km^3 yr^{-1} (MRC, 2005).

The Mekong's hydrological regime, with its annual flood pulse, has created a river basin rich in biodiversity (Junk et al., 2006) with highly productive aquatic ecosystems (Lamberts, 2008). These aquatic ecosystems support one of the world's richest inland fisheries (Baran and Myschowoda, 2009) and are the source of livelihoods and food for millions of people (Hortle, 2007; MRC, 2010). Intra-annual variation between wet and dry periods has also shaped the region's

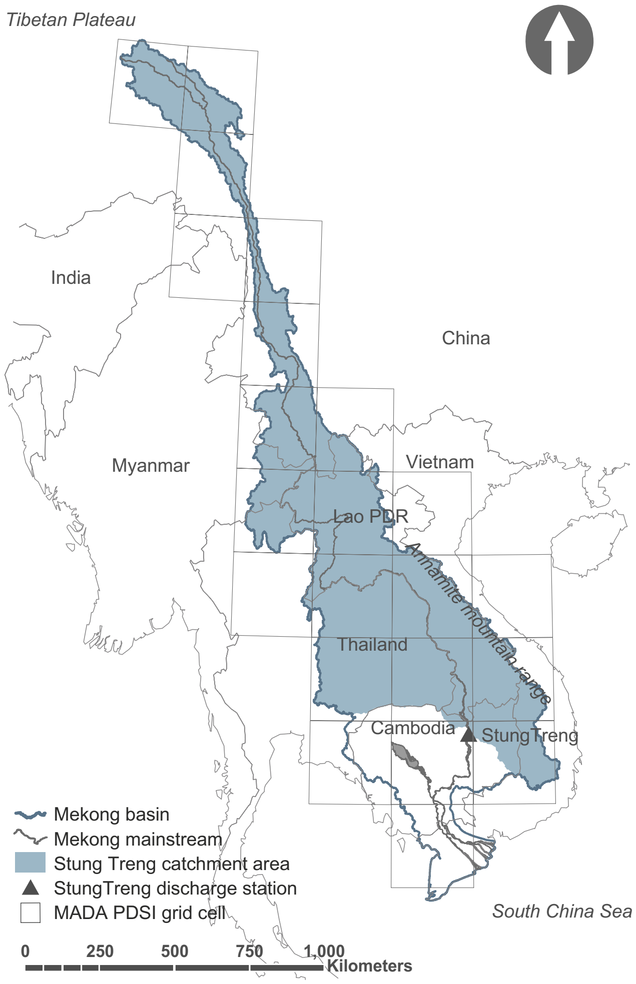

Fig. 1. The Mekong River basin and the MADA PDSI grid cells (Cook et al., 2010) used in this study. The blue shaded area is the catchment area for the Stung Treng discharge measurement station.

agriculture, which is the single most important livelihood in the Mekong Region (MRC, 2010). The region's food production and livelihoods have co-developed with the monsoon climate and are therefore susceptible to variations in it, for example, the timing, length, and magnitude of the monsoon season and flood pulse affect agricultural production (MRC, 2010; Chinvanno et al., 2008) as well as fishing (Baran and Myschowoda, 2009).

2.2 Past research

Recent research concludes that the variability of Mekong discharge has increased during the 20th century. Delgado et al. (2010) found that the variability in flows and likelihood of extreme floods increased during the last half of the 20th century, whilst the probability of average floods decreased. The increase in variability is linked to changes in the western North Pacific Monsoon (WNPM) (Delgado et al., 2012), which has become more variable since the late 1970s (Wang et al., 2001). The WNPM is coupled with ENSO (Wang et al., 2008), whose magnitude and periodicity have increased since the late 1970s (Wang et al., 2008). Although there are clear indicators of a recent increase in hydrological variability in the Mekong, there is no comprehensive understanding of whether this recent variability falls within the normal long-term range of variability. Moreover, in their research, Delgado et al. (2010, 2012) used observed discharge, which may be affected by direct human activities, such as irrigation, reservoir operation and land cover changes.

In mainland Southeast Asia there are few studies focusing on long-term climate variability (Buckley et al., 2007, 2010; Fan et al., 2008; Sano et al., 2009; Fang et al., 2010; Cook et al., 2010). With the exception of the study by Buckley et al. (2007), these are based on a methodology where tree ring chronologies are used to reconstruct past climates using the Palmer Drought Severity Index (PDSI). The study by Buckley et al. (2007) did not use PDSI in the reconstruction, and focused mainly on interpreting the tree ring chronology. The common finding of these studies is that of multi-year or decadal scale variations in climate. The studies listed above cover varying geographical regions and time periods; do not investigate climate variability at the river basin scale; and do not address the recent changes in climate variability in light of the longer time perspective. In this paper we aim to apply our newly developed approach to bridge these two groups of studies (recent variability studies based on discharge and palaeoclimate studies based on tree ring chronologies).

3 Data and methodology

The development of the approach to assess the long-term variability of hydrometeorological conditions and discharge at the river basin scale is based on three parts: (i) calculation of basin averaged PDSI from MADA (Cook et al., 2010); (ii) comparison of basin averaged PDSI with discharge; and (iii) long-term analysis of hydrometeorological variability. The development of the approach was carried out using the Mekong River basin as a case study, but the approach itself is intended to be applicable to other river basins in Asia covered by MADA. The data and methodologies used in the analysis of the case study area are described in the following sections.

3.1 Data

The original PDSI data in MADA were reconstructed by Cook et al. (2010) using tree ring records from more than 300 sites in Asia, together with a gridded PDSI dataset (Dai et al., 2004). The resulting MADA is a seasonalised gridded PDSI dataset for the summer (June-July-August) with a 2.5° spatial resolution, covering Monsoon Asia over the period 1300–2005. The method for reconstruction of the gridded dataset was based on a point by point regression method.

PDSI is a widely used index for describing meteorological drought and wetness (Heim, 2002; Dai et al., 2004), and was originally developed by Palmer (1965). The PDSI is based on precipitation and temperature, which are used in the calculation of atmospheric moisture demand at the soil surface. A major benefit of the PDSI in long-term climate and hydrometeorological analyses is that it is based on meteorological factors and thus reflects only the variations in climate, excluding the potential influences of land use changes, dam construction, and irrigation, which may be contained, for example, in discharge data. In general, MADA provides an important means for understanding climate in Monsoon Asia and it has already proven to be useful for this purpose (Wahl and Morrill, 2010; Bell et al., 2011). The MADA dataset was obtained from NOAA's palaeoclimatology online database (NOAA, 2010).

For our analyses we used the MADA PDSI dataset to derive basin averaged PDSI for the entire Mekong Basin ($PDSI_M$) and for the part of the basin upstream from Stung Treng measurement station ($PDSI_{ST}$), being a reliable downstream station before the Cambodian floodplains (see location in Fig. 1). The catchment area upstream from Stung Treng covers 79 % of the Mekong Basin. The $PDSI_{ST}$ and $PDSI_M$ were calculated as area weighted sums of the MADA PDSI grid cells that are fully or partly inside the specific catchment area (see location of used MADA grid cells in Fig. 1). This resulted in two time series, $PDSI_M$ and $PDSI_{ST}$, describing the summer (June-July-August) monsoon conditions of the Mekong basin and the Stung Treng catchment over the period 1300–2005.

Daily discharge data from Stung Treng were obtained from the Mekong River Commission's quality assured database (MRC, 2011c). The discharge data cover the period 1910–2005, but the period before 1952 is known to be less reliable (Erland Jenssen, Mekong River Commission, personal communication, 26 April 2010). This first part (1910–1952) of the time series is lacking a rating curve and the actual discharge has been calculated retrospectively with rating curves defined after the year 1952. Therefore, the first part of the time series may contain inaccuracies in flow volumes but we expected that the data still contain the interannual discharge variability. For the final analyses the daily discharge data were transformed into cumulative flows of hydrological years, which were defined as the beginning of May to the end of April of the next year, following Kummu and Sarkkula (2008). The cumulative flows of hydrological years were used as indicators for monsoon conditions similarly as the $PDSI_M$ and $PDSI_{ST}$. For the analysis of $PDSI_{ST}$, $PDSI_M$ and discharge of hydrological years, the data were standardised using standard scores.

3.2 Methods

Firstly, we compared the $PDSI_{ST}$ with the discharge measurements from Stung Treng over the period 1910–2005. In the comparison we used visual examination; local regression smoothing (LOESS) to examine patterns in long-term average conditions; moving window variance to visualise the changes in the total variance in time; the Levene type test for linear trends in variances to determine whether there are statistically significant increases in the total variances; continuous wavelet transform (CWT) to identify variability patterns and their temporal variations in frequency domain; and wavelet coherency (WCO) to examine the coherence of the variability patterns in $PDSI_{ST}$ and discharge in frequency domain. Secondly, we analysed the long-term hydrometeorological conditions of the Mekong Basin using $PDSI_M$ over the period 1300–2005. In the analysis of $PDSI_M$, we used LOESS smoothed data to identify prolonged dry and wet epochs; CWT to identify variability patterns and their temporal variations in frequency domain; moving window variance to visualise the changes in the total variance in time; and the Levene test for equality of variances to examine the changes in the total variances during the period 1300–2005. Below, these methods are briefly introduced.

3.2.1 LOESS smoothing

The local regression (LOESS) (Cleveland, 1979; Cleveland and Devlin, 1988) was used for smoothing the $PDSI_{ST}$, $PDSI_M$, and discharge time series. The purpose of the smoothing was to examine long-term patterns in average conditions. LOESS is a model that uses multiple regression models to fit a function on a time series with an n length subset of the time series data. By fitting the function on the original data, the result is a smoothed time series and the degree of smoothing depends on n. In this study we used $n = 21$, as it was found to adequately remove short-term variation and to reveal long-term patterns.

3.2.2 Tests for linear trends and homogeneity of variances

We used a Levene type of test for linear trend in group variances (Gastwirth et al., 2009) to define whether the $PDSI_{ST}$ and discharge at Stung Treng have trends in their variances in 1910–2005 period. The test was based on the Levene's test for equality of variances of two groups (Levene, 1960), but instead of two groups the test determines whether variances of several groups decrease or increase linearly. In our test we divided the data from the period 1910–2005 into eight groups ($n = 12$) and determined whether there is a linear trend in group variances. The original Levene's test was also modified to increase the robustness of the test by using group medians instead of group means as suggested by Brown and Forsythe (1974) and by computing bootstrap p values to adapt for the small number of data points ($n = 12$) as suggested by Lim and Loh (1996).

We also used the Levene's test for equality of group variances (Levene, 1960) to determine whether the $PDSI_M$

variance in the latest decades was higher than in other epochs within the 1300–2005 study period. For this we divided the $PDSI_M$ data into 50 yr periods and tested whether the last period (1956–2005) has the highest levels of variance, in a pair-wise manner, compared to each earlier 50 yr period. Here, again, we used group medians instead of means to increase the robustness of the test, as suggested by Brown and Forsythe (1974).

3.2.3 Continuous wavelet transform (CWT) and wavelet coherency (WCO)

The CWT was used to examine the recurring periodicities and their relative strength in the time series, similarly to the spectral analysis, but it also revealed the temporal localisation of these periodicities (Torrence and Compo, 1998). The WCO was used to assess the periodicities where two time series co-vary and also analyse the temporal localisation of these co-variations and their phase relationships. Both of these wavelet analyses were based on the Morlet wavelet function with standard parameterisation from the wavelet package developed by Grinsted et al. (2004). The wavelet analyses were also complemented with variance analysis with a 21 yr moving window. The statistical significances of the variation in CWT and co-variation in WCO were tested with a 5 % significance level. The null-hypothesis for the significance test is that the data are normally distributed and can be sufficiently described with the first order autoregressive model (AR(1)). Therefore, prior to carrying out the CWT and WCO analyses the normality and AR(1) assumptions were examined using the Shapiro–Wilk test (Shapiro and Wilk, 1965) and partial autocorrelation plots with 5 % significance levels. The AR(1) assumption in significance testing is important for CWT but less so for WCO (Grinsted et al., 2004). The WCO further shows the phase relationships of two time series (i.e. the potential timing difference) with arrows: $\rightarrow$ in phase; $\leftarrow$ anti phase; $\uparrow$ discharge leading $PDSI_{ST}$ by 90°; and $\downarrow$ $PDSI_{ST}$ leading discharge by 90°.

3.2.4 Identification of prolonged wet and dry epochs

The wet and dry epochs of multi-annual lengths were identified using LOESS smoothed $PDSI_M$ time series. Dry epochs were defined as periods when smoothed PDSI values are below -0.44, and wet epochs as periods when smoothed PDSI values are above 0.44. These thresholds correspond approximately to the upper and lower 15 % percentiles of the data, similarly as the standardised annual PDSI values of 1 and -1 represent the boundaries for upper and lower 15 % percentiles. The PDSI value -1 ($+1$) is commonly used to indicate the threshold for moderate drought (wet spell), but it is dependent on region specific standardisation of the index (Alley, 1984). The resulting definition is somewhat arbitrary but it is expected to serve the purpose of approximating the major dry and wet epochs in a palaeoclimatological context.

Furthermore, we identified very wet and very dry individual years in annual $PDSI_M$ data using thresholds of 2 and -2 (i.e. two standard deviations), which are generally used to indicate severe drought and wet spells (Alley, 1984). It is worth noting that the traditional definition of drought does not apply here, as the MADA describes the conditions of the wet monsoon months.

4 Results of the Mekong Basin case study

4.1 The comparison of $PDSI_{ST}$ and discharge at Stung Treng

To explore how the PDSI represents discharge in the Mekong, we compared the $PDSI_{ST}$ and discharge at Stung Treng over the period 1910–2005 (Fig. 2a). The annual values of $PDSI_{ST}$ and discharge show a statistically significant correlation of 0.47 ($p < 0.001$), but some differences exist. The $PDSI_{ST}$ peaks seem to match the discharge peaks better in the post-1935 period, when the correlation was 0.56 ($p < 0.001$). The correlation in the pre-1935 period was statistically not significant. It seems that in the pre-1935 period, $PDSI_{ST}$ and discharge have similar patterns in their variation but there is a timing difference between them: $PDSI_{ST}$ is leading discharge by two years. This was verified by deleting the years 1937 and 1938 from $PDSI_{ST}$ and moving the pre-1935 $PDSI_{ST}$ data two years forward in time. By this adjustment the correlation of the pre-1935 period was 0.38 ($p = 0.058$) and the correlation of 1910–2005 was 0.51 ($p < 0.001$). This adjustment of $PDSI_{ST}$ was done here to illustrate the timing difference and the rest of the analyses in this paper are performed with the original $PDSI_{ST}$ and $PDSI_M$.

When $PDSI_{ST}$ and discharge were smoothed with LOESS over the period 1910–2005, both time series showed similar patterns (Fig. 2a). The smoothing reveals that the period from the 1920s to the late 1950s was wetter than average, and the period from the 1970s to late 1990s was drier than average. The moving variances with a 21 yr moving window show that the variance of $PDSI_{ST}$ and discharge follow similar patterns, and that the variances have increased during the 1910–2005 period (Fig. 2b). The Levene type test for linear trends in variances confirmed the increased variance, both in $PDSI_{ST}$ and discharge ($p < 0.01$).

The CWT of $PDSI_{ST}$ and discharge over the period 1910–2005 show that both variables have recurring periodicities with wavelengths of 4–7, 10–14, and 19–30 yr (Fig. 3a, b). The periodicities on wavelengths of 4–7 yr were stronger both in $PDSI_{ST}$ and discharge during the 1910s–1930s, 1950s–1970s, and from the 1980s onwards, while the periodicity of 10–14 yr was the strongest between the 1930s and 1960s. The periodicity of 19–30 yr is outside the cone of influence of the wavelet analysis, and therefore should not be considered. An interesting feature in the CWT results is that

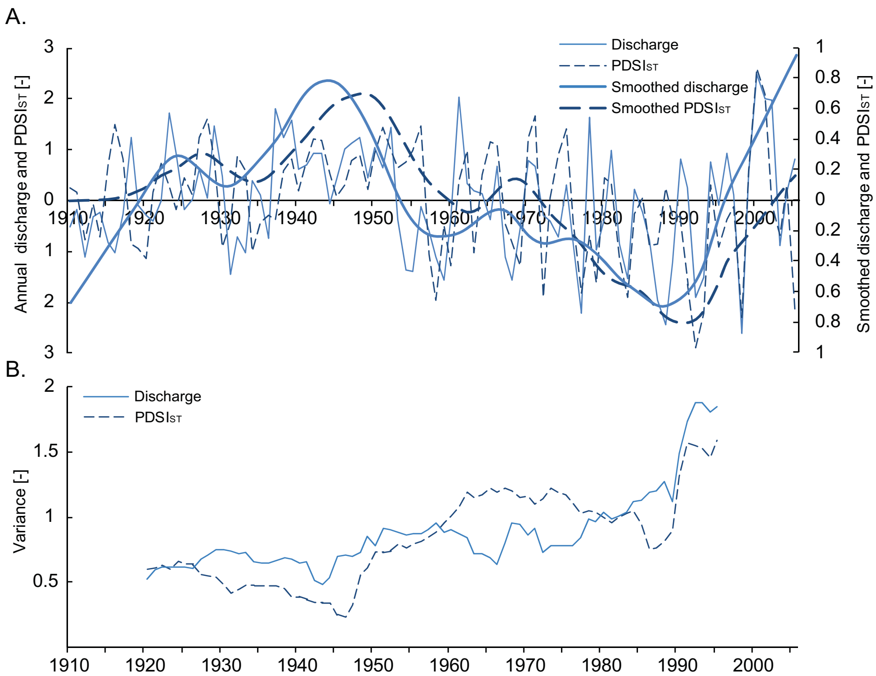

Fig. 2. Comparison of standardised basin averaged PDSI ($PDSI_{ST}$) and discharge for Stung Treng over the period 1910–2005: **(A)** annual values and LOESS smoothed values; and **(B)** moving variances with a 21 yr window.

both $PDSI_{ST}$ and discharge showed a remarkable increase in periodicities of 2–7 yr in the post-1950 period (Fig. 3a and b, respectively), which are also known to be the wavelengths for ENSO variability. The increase in periodicities on wavelengths of 2–7 yr at least partly explains the increased variance in the 1910–2005 period detected by the Levene type test for linear trends variances. It is important to note that the statistically significant areas for discharge shown by the CWT (areas marked with black line in Fig. 3a) must be viewed with caution as the partial autocorrelation plot showed a significant peak at lag 5, suggesting the discharge to be AR(5) process, which is against the AR(1) assumption of the significance testing.

WCO conducted for $PDSI_{ST}$ and discharge confirms that the two time series co-vary in multiple frequencies (Fig. 3c). Significant co-variation can be observed in WCO at wavelengths of 2–7, 10–14, and 19–30 yr (Fig. 3c). When the WCO (Fig. 3c) is compared with CWT of $PDSI_{ST}$ and discharge (Fig. 3a, b), it can be observed that both $PDSI_{ST}$ and discharge have regions with high power coinciding with the areas of co-variation. Strong co-variation with high powers can be observed especially on wavelengths of 2–7 yr.

The phase arrows in the WCO (Fig. 3c) indicate that the phase relationship between $PDSI_{ST}$ and discharge was not constant during the period of 1910–2005. For example, the phase arrows at wavelengths of 4–7 yr show change from $PDSI_{ST}$ leading the discharge in the pre-1935 period to a more in-phase relationship for the rest of the study period. This indicates a timing difference between the $PDSI_{ST}$ and discharge time series in the early part of the time series. The same timing difference can also be observed in the plotted annual $PDSI_{ST}$ and discharge data (Fig. 2a), where the $PDSI_{ST}$ and discharge show clear resemblance in their patterns in the pre-1935 period, as the peaks in $PDSI_{ST}$ are leading the discharge by two years.

4.2 Palaeological time scale hydrometeorological variability in the Mekong

As shown in Sect. 4.1, a statistically significant relationship was found between $PDSI_{ST}$ and the Mekong's discharge at Stung Treng. Therefore, the $PDSI_M$ is expected to be a good proxy for the whole Mekong basin's hydrometeorology for the period 1300–2005. The $PDSI_M$ for that period shows clear prolonged wet and dry epochs in the Mekong's hydrometeorology (Fig. 4a). The most distinguishable dry and wet epochs are listed in Table 1. The recent dry epoch of 1977–1995 and the wet epoch of 1938–1955 were the most significant epochs in the whole 1300–2005 period in terms of their magnitude. The post-1950 period shows a considerable number of very dry years with ($PDSI_M < -2$) while the wet years ($PDSI_M > 2$) are more evenly distributed over the study period (Table 1, Fig. 4a). The two wettest years during the whole study period occurred, however, in 2000 and 2001 (Table 1, Fig. 4a).

The CWT (Fig. 4b) of the $PDSI_M$ revealed highly volatile features in the Mekong's hydrometeorology. Five periods with different variation characteristics can be identified. First

Table 1. Prolonged wet and dry epochs and individual dry and wet years in the Mekong Basin according to basing averaged PDSI ($PDSI_M$) derived from the Monsoon Asia drought Atlas (MADA). The wet and dry epochs were defined from smoothed $PDSI_M$ with values above 0.44 or below −0.44, respectively. These limits correspond to 15 % upper and lower percentiles. The individual dry and wet years were defined as $PDSI_M$ values above 2 and below −2, which correspond to 2.5 % upper and lower percentiles.

	Range of years/individual years
Dry epochs	1344–1365, 1405–1407, 1418–1423, 1479–1490, 1608–1610, 1630–1640, 1645–1648, 1670–1682, 1755–1769, 1870–1871, 1898–1902, 1977–1995
Individual dry years	1609, 1629, 1634, 1635, 1837, 1958, 1972, 1977, 1983, 1991, 1992, 1993, 1998, 2005
Wet epochs	1509–1520, 1586–1597, 1618–1625, 1655–1664, 1711–1734, 1781–1782, 1804–1811, 1925–1929, 1938–1955, 2003–onwards
Individual wet years	1375, 1511, 1600, 1625, 1657, 1662, 1713, 1715, 1730, 1780, 1808, 1809, 1829, 1861, 1928, 1951, 1971, 2000, 2001

is the 1300–1575 period, with relatively low variability and dominant periodicities at wavelengths of 50–83 yr. The second period, 1575–1680, has dominant periodicities with wavelengths of 4–6 and 15–38 yr. The third period, 1680–1780, is characterised again by dominant periodicities above 50 yr. The fourth period, 1780–1900, is characterised by dominant periodicities in wavelengths of 4–7 yr. The fifth and last period, 1900–2005, is characterised by dominant periodicities in wavelengths of 4–7, 11–15, and above 50 yr. The second half of the fifth period clearly stands out from the whole study period with high variability at multiple wavelengths. Although the differences in variability between the five periods can be reliably observed from the CWT (Fig. 4b), the statistical significance test must be viewed with caution as the $PDSI_M$ data were found to be closer to an AR(2) process than AR(1).

The results from the moving window variance support the CWT findings revealing varying variability in hydrometeorological conditions over the 1300–2005 period (Fig. 4c). The most distinct increases in variability were observed during the 1575–1680 and 1950–2005 periods. The last period, 1950–2005, showed the highest levels of variability, particularly in the post-1950 period, which are not observed elsewhere in the study period. The Levene test for equality of variances confirmed that the variance in the post-1950 period was higher than the variance in any of the earlier 50 yr periods (Table 2).

Table 2. The variances and statistical significance of the Levene test for equality of variances for the 50 yr periods of $PDSI_M$. The variance of each 50 yr period (within 1306–1955) was tested against the variance of the period 1956–2005 in a pair-wise manner. Small *p* values suggest that the variance of a particular period was significantly lower than the variance of the period 1956–2005.

Period	Variance	*p* value
1306–1355	0.64	< 0.001
1356–1405	0.79	< 0.001
1406–1455	0.58	< 0.001
1456–1505	0.64	< 0.001
1506–1555	0.50	< 0.001
1556–1605	0.69	< 0.001
1606–1655	1.29	0.006
1656–1705	0.94	< 0.001
1706–1755	1.05	0.003
1756–1805	0.74	< 0.001
1806–1855	1.09	0.004
1856–1905	0.92	0.001
1906–1955	0.85	< 0.001
1956–2005	2.85	–

5 Discussion

5.1 Basin-wide MADA PDSI approach

In this article we developed an approach for assessing the river basin-wide hydrometeorological and discharge variability on a palaeological time scale. The approach was tested in the Mekong basin and it proved to be successful, especially in describing prolonged dry and wet epochs and changes in the interannual variability of the hydrometeorological conditions and discharge. The approach is based on basin averaged PDSI derived from MADA (Cook et al., 2010), which is then validated with measured discharge of a basin in question. The approach is not site specific but can be applied in other river basins covered by MADA.

Dai and Trenberth (1998) and Dai et al. (2004) also found that basin averaged PDSI is a good proxy for streamflow in their analysis of seven of the world's largest river basins. They found correlations varying from 0.6 to 0.8 between basin-averaged PDSI and streamflow (Dai et al., 2004), whereas the correlation in our approach was 0.47. However, Dai et al. (2004) used instrumental data, and did not use palaeological proxy data to extend the analyses to cover longer time scales. Moreover, they did not investigate in detail how well the basin-wide PDSI corresponds with the discharge, or what kind of variability characteristics the basin-wide PDSI contains.

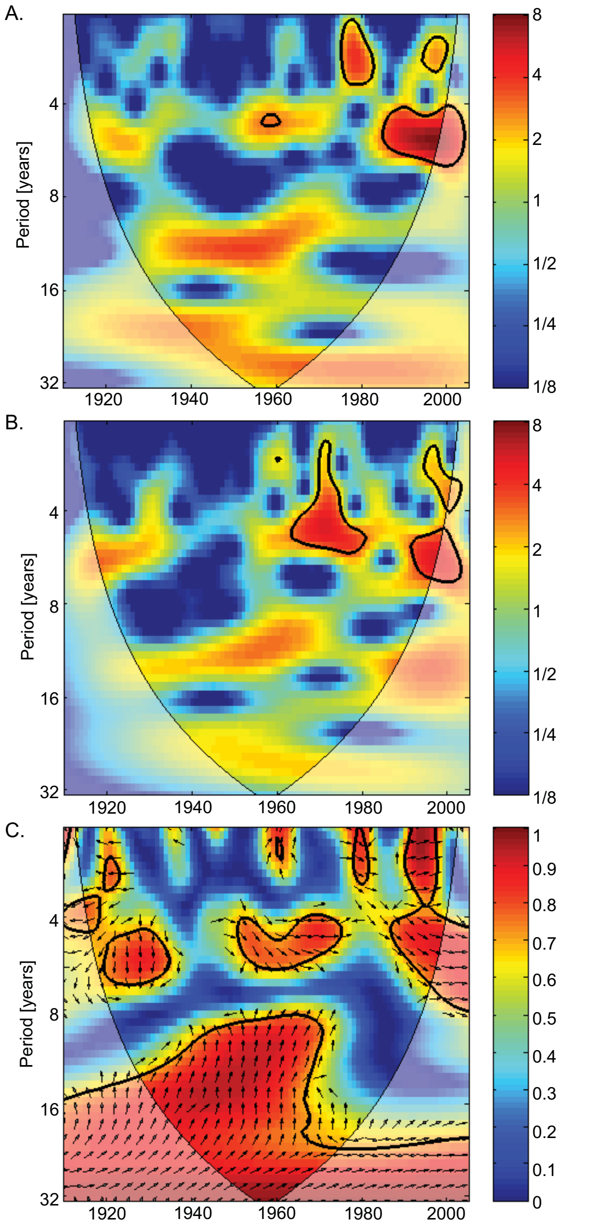

Fig. 3. Comparison of basin averaged PDSI for Stung Treng catchment area ($PDSI_{ST}$) and discharge at Stung Treng measurement station over the period of 1910–2005 in frequency domain: **(A)** continuous wavelet transforms (CWT) for discharge; **(B)** CWT for $PDSI_{ST}$; and **(C)** wavelet coherency (WCO) of discharge and $PDSI_{ST}$. In tiles A and B, the increase in the power of the signal is shown in colour change from blue towards red and in tile C the colour change from blue towards red indicates increasing coherence between $PDSI_{ST}$ and Q_{ST}. Statistically significant (5 %) areas are marked with a black line. The significance test for discharge (tile A) must be viewed with caution since the assumptions of the test are not fully met as the discharge was found to follow an AR(5) process which is against the AR(1) assumption. The arrows in tile C indicate the phase difference (i.e. timing difference) between $PDSI_{ST}$ and discharge: → in phase; ←anti phase; ↑ discharge leading $PDSI_{ST}$ by 90°; and ↓ $PDSI_{ST}$ leading discharge by 90°.

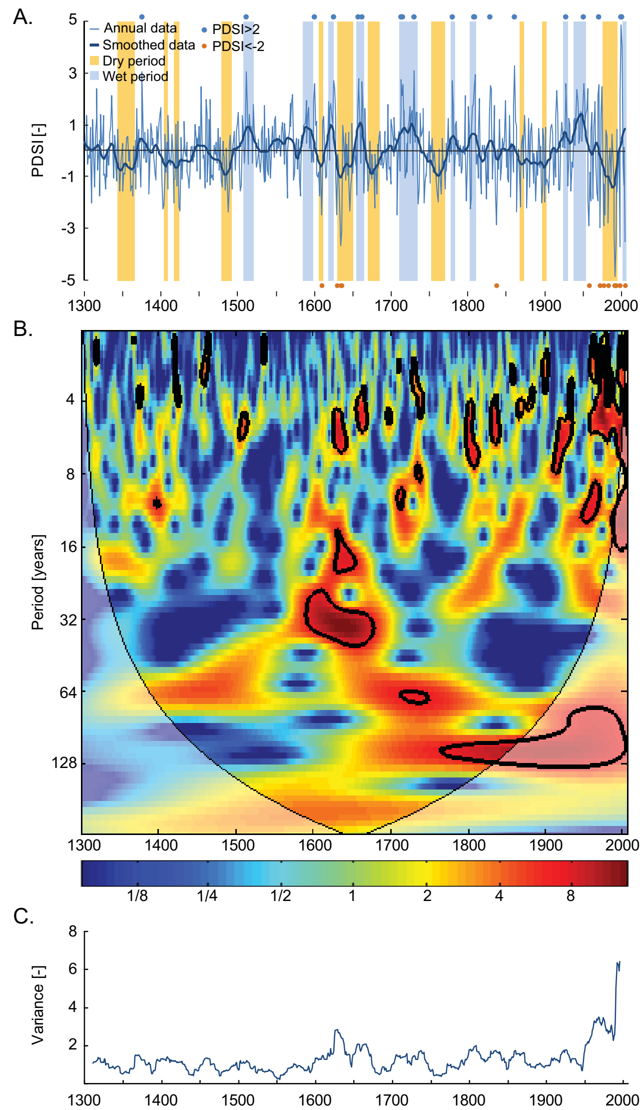

Fig. 4. Long-term periodicity: **(A)** basin averaged PDSI of the Mekong ($PDSI_M$) for the period 1300-2005; **(B)** continuous wavelet transform (CWT); and **(C)** moving variance of the $PDSI_M$. In tile A, the thin blue line represents annual values of $PDSI_M$, while the thick blue line represents the smoothing with LOESS; positive (negative) PDSI values refer to wet (dry) years. The dots in tile A represent the years when $PDSI_M$ values are larger than 2 or smaller than −2. Prolonged dry and wet periods are also shown in tile A with blue (wet) and orange (dry) shadings. In tile B, an increase in the power of the periodicities is marked with a colour change from blue to red and statistically significant periodicities (significance level 5 %) are marked with a black line. The significance test of CWT (tile B) must be viewed with caution since the assumptions of the test are not fully met as the $PDSI_M$ was found to follow AR(2) process which is against the AR(1) assumption.

The use of PDSI in long-term drought trends has been criticised by Sheffield et al. (2012). They found that standard PDSI might give biased estimates on drought trends due to the simplistic formulation of potential evaporation (PE) in standard PDSI. They argue that more physically based methods should be used for defining PE. The MADA, however, describes the wet monsoon conditions of June-July-August when the variability is driven mainly by rainfall, and therefore it is not clear how significant the findings of Sheffield et al. (2012) are for MADA. Furthermore, in the basin-wide approach developed here we focused on interannual variability (i.e. relatively short-term changes), which is not expected to be affected by the findings of Sheffield et al. (2012) on long-term trends in average conditions.

5.2 Basin-wide MADA PDSI approach for the Mekong

The comparison of $PDSI_{ST}$ and discharge at Stung Treng (see Sect. 4.1) suggested that the basin averaged PDSI derived from MADA (Cook et al., 2010) can be used as a proxy for the interannual variability and long-term average conditions of the Mekong main stem discharges. Both the $PDSI_{ST}$ and discharge had similar long-term patterns in average conditions (Fig. 2a). At an annual scale, the $PDSI_{ST}$ was found to be a less robust proxy due to lower correlations and timing difference between $PDSI_{ST}$ and discharge in the pre-1935 period. The CWT and WCO analyses of $PDSI_{ST}$ and discharge (Fig. 3) also revealed that they both contain similar variability characteristics at several wavelengths.

The visual examination and WCO analysis of $PDSI_{ST}$ and discharge also revealed a phase difference where the $PDSI_{ST}$ was leading discharge by 2 yr. To confirm the quality of the discharge data we compared the discharge measurements from Stung Treng with discharge measurement from an upstream station at Pakse over the period 1923–2005, and did not find any phase shifts between these two stations. The reasons for the phase shift in the pre-1935 period could not be further investigated, as there are no further hydrological data available to compare with the PDSI data in early 20th century. The phase difference does not, however, compromise the use of the developed approach as a proxy for prolonged dry and wet periods of interannual discharge variability in a palaeological context. This is because the phase difference was only a two year timing difference between the discharge and $PDSI_{ST}$ data, and otherwise the data showed good resemblance and correlation in time (Fig. 2) and frequency domains (Fig. 3). But we suggest that great care should be taken if the developed basin-wide approach should be used as a proxy for discharges on annual resolution in time domain. The timing differences, at least, should be thoroughly investigated.

The analyses carried out for the $PDSI_M$ for the period 1300–2005 revealed that the hydrometeorological conditions of the Mekong have varied between prolonged wet and dry epochs. The most recent epoch was one of the driest and had several extremely dry years. The wet and dry epochs have been reported earlier in the literature regarding mainland Southeast Asia by Buckley et al. (2007), Fan et al. (2008), Sano et al. (2009), Buckley et al. (2010), Fang et al. (2010), and Cook et al. (2010). They report several distinct dry and wet epochs, many of which coincide with our findings, for example the dry epochs of the 1340s–1360s, 1750s–1760s, 1870s, and 1970s–1990s, and the wet epochs of the 1500s–1520s, 1580s–1590s, 1610s–1620s, 1710s–1730s, and 1930s–1950s (see Fig. 4a and Table 1). Shorter but severe well-known drought epochs can also be observed from the $PDSI_M$ dataset, such as the Strange Parallels drought of 1756–1768 and the late Victorian Drought of 1876–1878 (Cook et al., 2010). The droughts associated with the known historical El Niño events of 1877–1878, 1888–1889 and 1918–1919 (Cook et al., 2010; Buckley et al., 2010) are also clearly visible in $PDSI_M$ (Fig. 4a). It should be noted, however, that the above studies focused on smaller regional scales or in different locations in mainland Southeast Asia and none of them analysed these dry and wet epochs at a river basin scale. Neither did they focus on changes in interannual variability of hydrometeorological conditions.

The $PDSI_M$ also suggested that the post-1950 period has experienced a significant increase in the occurrence of dry years ($PDSI < -2$) (Fig. 4a). The literature also reports significant drought years in recent decades. For example, significant meteorological or hydrological droughts were experienced in 1992, 1993, 1998, 1999, and 2003–2005 (Te, 2007; MRC, 2010). The $PDSI_M$ data agree with these findings for most of those years. The years 1992, 1993, 1998, 2003, and 2005 ranked as the 1st, 4th, 2nd, 97th, and 5th driest years, respectively, over the whole period 1300–2005.

The analyses on $PDSI_{ST}$ and $PDSI_M$ also revealed that the interannual variability has increased in recent decades, and that the level of variability in the post-1950 period was the highest experienced during the entire study period (Fig. 4c and Table 2). This finding is in line with the findings of Delgado et al. (2010, 2012), who found increased discharge variability in the second half of 20th century. Much of the increased variability observed in $PDSI_{ST}$ and $PDSI_M$ occurred in ENSO wavelengths of 2–7 yr (Figs. 3 and 4b). Therefore, we further used Multivariate ENSO Index (MEI.ext) (Wolter and Timlin, 2011) to investigate the relationship between ENSO and $PDSI_{ST}$ and discharge.

5.3 The role of ENSO in increased hydrometeorological and discharge variability in the Mekong

We performed CWT on average December-January-February months of MEI.ext (MEI_{DJF}) and WCO between MEI_{DJF} and discharge and MEI_{DJF} and $PDSI_{ST}$ (Fig. 5). The December-January-February months of ENSO have been found to correlate well with the Mekong's discharge (Räsänen and Kummu, 2013) and have also been used in long-term and large scale analyses of ENSO variability

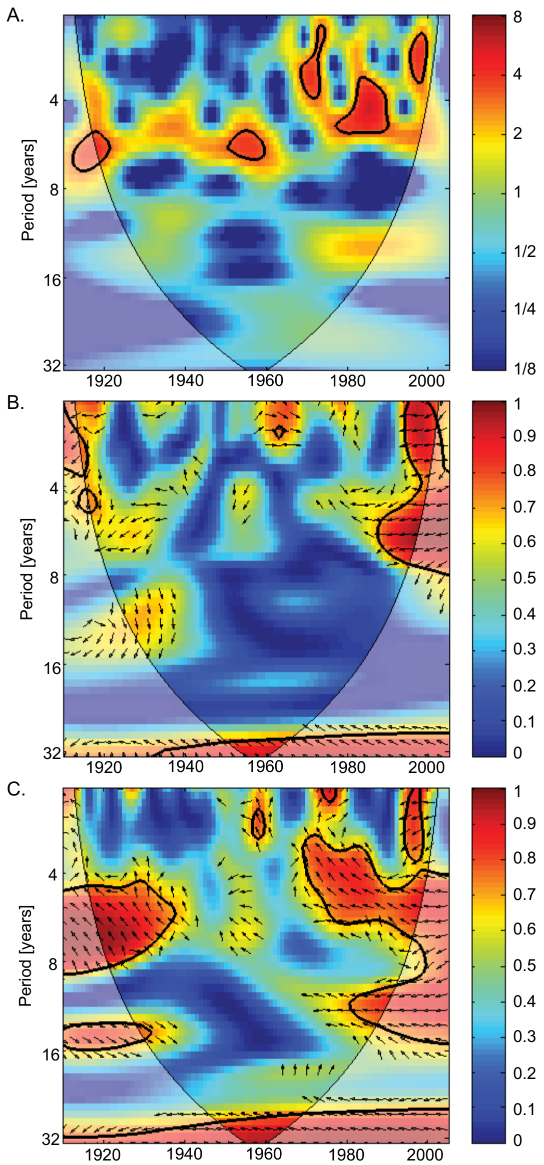

Fig. 5. Comparison of the relationship of discharge and basin averaged PDSI for Stung Treng catchment area ($PDSI_{ST}$) to December-January-February average of the Multivariate El Niño Southern Oscillation Index (MEI_{DJF}): **(A)** continuous wavelet transform (CWT) of MEI_{DJF}; **(B)** wavelet coherency (WCO) of discharge and MEI_{DJF}; and **(C)** WCO of $PDSI_{ST}$ and MEI_{DJF}. In tile A, the increase in the power of the signal is shown in colour change from blue towards red and in tiles B and C the colour change from blue towards red indicates increasing coherence between $PDSI_{ST}$ and Q_{ST}. Statistically significant (5 %) areas are marked with a black line. The significance test of CWT (tile A) must be viewed with caution since the assumptions of the test are not fully met as MEI_{DJF} was found to follow an AR(5) process which is against the AR(1) assumption. The arrows in tile C indicate the phase difference (i.e. timing difference) between $PDSI_{ST}$ and discharge: → in phase; ←anti phase; ↑ discharge leading $PDSI_{ST}$ by 90°; and ↓ $PDSI_{ST}$ leading discharge by 90°.

(D'Arrigo et al., 2005; Ward et al., 2010). The CWT of MEI_{DJF} (Fig. 5a), WCO between MEI_{DJF} and discharge (Fig. 5b), and WCO between MEI_{DJF} and $PDSI_{ST}$ (Fig. 5c), suggest that much of the variability in $PDSI_{ST}$ and discharge on wavelengths of 2–7 yr is associated with ENSO activity. These ENSO periods with high power (Fig. 5a) coincide rather well with the periods with high power in the CWT of $PDSI_{ST}$ and discharge (see Fig. 3a, b). The WCOs (Fig. 5b, c) confirm ENSO's relationship with $PDSI_{ST}$ and discharge. Significant co-variation can be observed especially around the 1920s and from the 1970s onwards, but the $PDSI_{ST}$ seem to have somewhat stronger coherence with ENSO than the discharge. CWT and WCOs related to ENSO (Fig. 5) also reveal that the periodicities with wavelengths of 2–4 yr have increased in the post-1960 period, suggesting increased ENSO related variability in the Mekong. The linear correlations also support this finding. The correlation between MEI_{DJF} and discharge, and MEI_{DJF} and $PDSI_{ST}$, for the period 1910–2005 were −0.31 ($p = 0.010$) and −0.44 ($p < 0.001$), respectively. In the 1980–2005 period, when the ENSO signal in the Mekong became more significant, the correlations between MEI_{DJF} and discharge and MEI_{DJF} and $PDSI_{ST}$ were −0.66 ($p < 0.001$) and −0.65 ($p < 0.001$), respectively.

The findings on ENSO–Mekong relationship are in line with the findings of Räsänen and Kummu (2013) and Darby et al. (2013), who found strengthened ENSO discharge relationship in the post-1980 period in the Mekong. ENSO is also known to have become more variable in the most recent decades (Yu et al., 2012; D'Arrigo et al., 2005; Cobb et al., 2013). The $PDSI_M$ further revealed high levels of interannual variability in the early 1700s (Fig. 4c) and this variability was associated partly to ENSO wavelengths (Fig. 4b). The early 1700s period is known to have experienced increased ENSO activity (D'Arrigo et al., 2005). Altogether, the findings suggest that the basin averaged PDSI derived from MADA is a good proxy for climate variability induced by ENSO, and much of the increased variability of the recent decades is associated with increased ENSO activity (Fig. 4b).

5.4 Future research directions

The basin-wide approach developed in this paper proved to be a suitable approach for studying the long-term hydrometeorological variability in the Mekong River basin. The MADA dataset (Cook et al., 2010), which our approach is partly based on, covers the whole of monsoon Asia and therefore our approach can be easily transferred to other river basins in the region. There are, however, some issues that could be further examined and developed in our approach, based on the experience from the Mekong. Firstly, the original MADA is derived from a set of tree ring chronologies with heterogeneous temporal coverage, which means that fewer tree ring chronologies have been used as predictors for PDSI in the earlier parts of the data period (Cook et al., 2010).

Therefore, it should be further examined whether the heterogeneous temporal distribution of predictors affects the variance characteristics in MADA. Secondly, although ENSO was captured well by the approach, it should be studied further to understand how well it captures the variability of other known atmosphere and ocean related oscillations, such as Pacific Decadal Oscillation and Indian Ocean Dipole, and the different components of the Asian monsoon. Thirdly, the MADA could be investigated at a single grid scale to understand how well it describes more localised hydrometeorological conditions. Fourthly, the developed basin-wide approach could contribute to future climate change studies by bringing a broader time perspective to the analyses and by providing a means for studying the long-term discharge variability. For example, there has been limited evidence on climate change induced discharge variability (IPCC, 2012), and future climate change projections often suggest large uncertainties in the direction of climate change impacts on river discharges (e.g. in the Mekong see, Kingston et al., 2011; Lauri et al., 2012).

6 Conclusions

In this paper, our aim was to develop an approach based on the Monsoon Asia Drought Atlas (MADA) for examining the recent interannual variability of hydrometeorological conditions and river discharge, at a river basin scale, in the perspective of long-term variability. To achieve that, we developed a basin-wide Palmer Drought Severity Index (PDSI) from MADA, validated this index with measured discharge, and examined the variability of hydrometeorological conditions and river discharge in a palaeoclimatological context over the period of 1300–2005. For this, we used the Mekong River basin as a case study area.

We found the basin-averaged PDSI derived from MADA to be a good proxy for detecting patterns in interannual variability and long-term average discharge conditions in the Mekong. Our approach provides a tool for studying river basin hydrometeorology and river discharge on palaeological time scales in any large basin in Monsoon Asia. The approach contributes especially to an improved understanding of discharge variability, by providing a long-term time perspective in which recent and projected future climate changes can be placed.

Specific to the Mekong, our case study results showed that the Mekong's hydrometeorological conditions have varied at multi-annual, decadal and centennial scales during the study period of 1300–2005. A distinct feature of the Mekong's hydrometeorological conditions is that they have varied between wetter and drier epochs with multi-annual and decadal lengths. Furthermore, two periods of increased interannual variability between wet and dry years were discovered, distinct features being the high occurrence of very dry years. The first period occurred in the early mid-17th century and the second in the post-1950 period. The interannual variability during the latter period was significantly higher than elsewhere in the whole study period. The increased interannual variability is associated with increased ENSO activity on wavelengths of 2–7 yr, but other sources of variability and their role were not examined. In summary, the data show that the Mekong has experienced exceptional hydrological times during recent decades. If variability continues to increase, this could affect ecosystems and societal functions in the Mekong Basin. For example, the productivity of aquatic ecosystems and agriculture is closely linked to hydrometeorological variability, and moreover, the design of existing infrastructure is based on past, observed, climate conditions.

Acknowledgements. The authors would like to thank the Mekong River Commission, particularly Erland Jensen, for kindly providing the discharge data for the study. The authors are grateful to Prof. Olli Varis, Marko Keskinen, Mirja Kattelus, Miina Porkka, Aura Salmivaara and Suvi Sojamo for support and cheerful working environment. Three reviewers and editor M. Sivapalan are highly acknowledged for their constructive comments that led to significant improvements in the paper. TR received funding from the RYM-TO Graduate School, MK from the postdoctoral funds of Aalto University, CL from the Maa- ja vesitekniikan tuki ry., and PJW received funding from a VENI grant from the Netherlands Organisation for Scientific Research (NWO).

Edited by: M. Sivapalan

References

Aerts, J. C. J. H., Renssen, H., Ward, P. J., De Moel, H., Odada, E., Bouwer, L. M., and Goosse, H.: Sensitivity of global river discharges under Holocene and future climate conditions, Geophys. Res. Lett., 33, L19401, doi:10.1029/2006GL027493, 2006.

Alley, W. M.: The Palmer Drought Severity Index: Limitations and Assumptions, J. Clim. Appl. Meteorol., 23, 1100–1109, 1984.

Anchukaitis, K. J., Buckley, B. M., Cook, E. R., Cook, B. I., D'Arrigo, R. D., and Ammann, C. M.: Influence of volcanic eruptions on the climate of the Asian monsoon region, Geophys. Res. Lett., 37, L22703, doi:10.1029/2010GL044843, 2010.

Baran, E. and Myschowoda, C.: Dams and fisheries in the Mekong Basin, Aquat. Ecosyst. Health, 12, 227–234, 2009.

Bell, A., Cook, B., Anchukaitis, K., Buckley, B., and Cook, E.: Repurposing climate reconstructions for drought prediction in Southeast Asia, Clim. Change, 106, 691–698, 2011.

Bogaart, P. W., Van Balen, R. T., Kasse, C., and Vandenberghe, J.: Process-based modelling of fluvial system response to rapid climate change II. Application to the River Maas (The Netherlands) during the last Glacial-Interglacial Transition, Quaternary Sci. Rev., 22, 2097–2110, 2003.

Brown, M. B. and Forsythe, A. B.: Robust Tests for the Equality of Variances, J. Am. Stat. Assoc., 69, 364–367, 1974.

Buckley, B., Palakit, K., Duangsathaporn, K., Sanguantham, P., and Prasomsin, P.: Decadal scale droughts over northwestern Thailand over the past 448 years: links to the tropical Pacific and Indian Ocean sectors, Clim. Dynam., 29, 63–71, 2007.

Buckley, B., Anchukaitis, K., Penny, D., Fletcher, R., Cook, E., Sano, M., Nam, L. C., Wichienkeeo, A., That Minh, T., and Mai Hong, T.: Climate as a contributing factor in the demise of Angkor, Cambodia, Proc. Natl. Acad. Sci. USA, 107, 6748–6752, 2010.

Chinvanno, S., Boulidam, S., Inthavong, T., Souvannalath, S., Lersupavithnapa, B., Kerdsuk, V., and Thi Hien Thuan, N.: Climate risks and rice farming in the lower Mekong river basin, in: Climate Change and Vulnerability, edited by: Leary, N., Conde, C., Kulkarni, J., Nyong, A., and Pulhin, J., Earthscan, 333–350, 2008.

Cleveland, W. S.: Robust Locally Weighted Regression and Smoothing Scatterplots, J. Am. Stat. Assoc., 74, 829–836, 1979.

Cleveland, W. S. and Devlin, S. J.: Locally Weighted Regression: An Approach to Regression Analysis by Local Fitting, J. Am. Stat. Assoc., 83, 596–610, 1988.

Cobb, K. M., Westphal, N., Sayani, H. R., Watson, J. T., Di Lorenzo, E., Cheng, H., Edwards, R. L., and Charles, C. D.: Highly Variable El Niño–Southern Oscillation Throughout the Holocene, Science, 339, 67–70, 2013.

Cook, E. R., Seager, R., Cane, M. A., and Stahle, D. W.: North American drought: Reconstructions, causes, and consequences, Earth-Sci. Rev., 81, 93–134, 2007.

Cook, E. R., Anchukaitis, K. J., Buckley, B. M., D'Arrigo, R. D., Jacoby, G. C., and Wright, W. E.: Asian Monsoon Failure and Megadrought During the Last Millennium, Science, 328, 486–489, doi:10.1126/science.1185188, 2010.

Coumou, D. and Rahmstorf, S.: A decade of weather extremes, Nat. Clim. Change, 2, 491–496, 2012.

D'Arrigo, R., Cook, E. R., Wilson, R. J., Allan, R., and Mann, M. E.: On the variability of ENSO over the past six centuries, Geophys. Res. Lett., 32, L03711, doi:10.1029/2004GL022055, 2005.

Dai, A. and Trenberth, K. E.: Global variations in droughts and wet spells: 1900–1995, Geophys. Res. Lett., 25, 3367–3370, 1998.

Dai, A., Trenberth, K. E., and Qian, T.: A Global Dataset of Palmer Drought Severity Index for 1870–2002: Relationship with Soil Moisture and Effects of Surface Warming, J. Hydrometeorol., 7, 1117–1130, 2004.

Darby, S. E., Leyland, J., Kummu, M., Räsänen, T. A., and Lauri, H.: Decoding the drivers of bank erosion on the Mekong river: The roles of the Asian monsoon, tropical storms, and snowmelt, Water Resour. Res., 49, 2146–2163, 2013.

Delgado, J. M., Apel, H., and Merz, B.: Flood trends and variability in the Mekong river, Hydrol. Earth Syst. Sci., 14, 407–418, doi:10.5194/hess-14-407-2010, 2010.

Delgado, J. M., Merz, B., and Apel, H.: A climate-flood link for the lower Mekong River, Hydrol. Earth Syst. Sci., 16, 1533–1541, doi:10.5194/hess-16-1533-2012, 2012.

Dobrovolny, P., Moberg, A., Brazdil, R., Pfister, C., Glaser, R., Wilson, R., van Engelen, A., Limanowka, D., Kiss, A., Halickova, M., Mackova, J., Riemann, D., Luterbacher, J., and Bohm, R.: Monthly, seasonal and annual temperature reconstructions for Central Europe derived from documentary evidence and instrumental records since AD 1500, Clim. Change, 101, 69–107, 2010.

Fan, Z.-X., Bräuning, A., and Cao, K.-F.: Tree-ring based drought reconstruction in the central Hengduan mountains region (China) since A.D. 1655, Int. J. Climatol., 28, 1879–1887, 2008.

Fang, K., Gou, X., Chen, F., Li, J., D'Arrigo, R., Cook, E., Yanng, T., and Davi, N.: Reconstructed droughts for the southeastern Tibetan Plateau over the past 568 years and its linkages to the Pacific and Atlantic Ocean climate variability, Clim. Dynam., 35, 577–585, 2010.

Fang, K., Gou, X., Chen, F., Davi, N., and Liu, C.: Spatiotemporal drought variability for central and eastern Asia over the past seven centuries derived from tree-ring based reconstructions, Quaternary Int., 283, 107–116, 2013.

Gastwirth, J. L., Gel, Y. R., and Miao, W.: The Impact of Levene's Test of Equality of Variances on Statistical Theory and Practice, Stat. Sci., 24, 343–360, 2009.

Grinsted, A., Moore, J. C., and Jevrejeva, S.: Application of the cross wavelet transform and wavelet coherence to geophysical time series, Nonlinear Proc. Geoph., 11, 561–566, 2004.

Heim, R. R.: A Review of Twentieth-Century Drought Indices Used in the United States, B. Am. Meteorol. Soc., 83, 1149–1165, 2002.

Hortle, K.: Consumption and the yield of fish and other aquatic animals from the lower Mekong Basin, Mekong River Commission Technical Paper 16, Mekong River Commission, Vientiane, available at: http://www.mrcmekong.org/assets/Publications/technical/tech-No16-consumption-n-yield-of-fish.pdf (last access: January 2012), 2007.

IPCC: Managing the Risks of Extreme Events and Disasters to Advance Climate Change Adaptation, A Special Report of Working Groups I and II of the Intergovernmental Panel on Climate Change, edited by: Field, C. B., Barros, V., Stocker, T. F., Qin, D., Dokken, D. J., Ebi, K. L., Mastrandrea, M. D., Mach, K. J., Plattner, G.-K., Allen, S. K., Tignor, M., and Midgley, P. M., Cambridge University Press, Cambridge, UK, and New York, NY, USA, 582 pp., 2012.

Junk, W. J., Brown, M., Campbell, I. C., Finlayson, M., Gopal, B., Ramberg, L., and Warner, B. G.: The comparative biodiversity of seven globally important wetlands: a synthesis, Aquat. Sci, 68, 400–414, 2006.

Kingston, D. G., Thompson, J. R., and Kite, G.: Uncertainty in climate change projections of discharge for the Mekong River Basin, Hydrol. Earth Syst. Sci., 15, 1459–1471, doi:10.5194/hess-15-1459-2011, 2011.

Kummu, M. and Sarkkula, J.: Impact of the Mekong River Flow Alteration on the Tonle Sap Flood Pulse, AMBIO, 37, 185–192, 2008.

Lamberts, D.: Little Impact, Much Damage: The Consequences of Mekong River Flow Alterations for teh Tonle Sap Ecosystem, in: Modern Myths of The Mekong, edited by: Kummu, M., Keskinen, M., and Varis, O., Water & Development Publications – Helsinki University of Technology, 3–18, 2008.

Lauri, H., de Moel, H., Ward, P. J., Räsänen, T. A., Keskinen, M., and Kummu, M.: Future changes in Mekong River hydrology: impact of climate change and reservoir operation on discharge, Hydrol. Earth Syst. Sci., 16, 4603–4619, doi:10.5194/hess-16-4603-2012, 2012.

Levene, H.: Robust Tests for Equality of Variances Stanford University Press, Palo Alto, 1960.

Lim, T.-S. and Loh, W.-Y.: A comparison of test of equality of variances, Comput. Stat. Data Anal., 22, 287–301, 1996.

MRC: Overview of the Hydrology of the Mekong Basin, Mekong River Commission., Vientiane Lao PDR, 73, 2005.

MRC: State of the Basin Report 2010, Mekong River Commission, Vientiane, Lao PDR, available at: http://www.mrcmekong.org/assets/Publications/basin-reports/MRC-SOB-report-2010full-report.pdf (last access: June 2012), 2010.

MRC: Flood Situation Report, November 2011, Technical Paper No. 36. Mekong River Commission, Vientiane, Lao PDR, available at: http://www.mrcmekong.org/assets/Publications/technical/Tech-No36-Flood-Situation-Report2011.pdf (last access: February 2012), 2011a.

MRC: Annual Mekong flood report 2010, Mekong River Commission, Vientiane, Lao PDR, available at :http://www.mrcmekong.org/assets/Publications/basin-reports/Annual-Mekong-Flood-Report-2010.pdf (last access: February 2012), pp. 76, 2011b.

MRC: Hydrological database, Mekong River Commission, Vientiane, Lao PDR, last access: November, 2011.

NOAA: Paleoclimatology, available at: http://www.ncdc.noaa.gov/paleo/paleo.html (last access: January 2012), 2010.

Notebaert, B., Verstraeten, G., Ward, P. J., Renssen, H., and Van Rompaey, A.: Modeling the sensitivity of sediment and water runoff dynamics to Holocene climate and land use changes at the catchment scale, Geomorphology, 126, 18–31, 2011.

Palmer, W. C.: Meteorological drought, Research paper 45, US Depart. of Commerce, 58 pp., 1965.

Räsänen, T. A. and Kummu, M.: Spatiotemporal influences of ENSO on precipitation and flood pulse in the Mekong River Basin, J. Hydrol., 476, 154–168, 2013.

Renssen, H., Lougheed, B. C., Aerts, J. C. J. H., De Moel, H., Ward, P. J., and Kwadijk, J. C. J.: Simulating long-term Caspian Sea level changes: the impact of Holocene and future climate conditions, Earth Planet. Sci. Lett., 261, 685–693, 2007.

Sano, M., Buckley, B., and Sweda, T.: Tree-ring based hydroclimate reconstruction over northern Vietnam from Fokienia hodginsii: eighteenth century mega-drought and tropical Pacific influence, Clim. Dynam., 33, 331–340, 2009.

Shapiro, S. S. and Wilk, M. B.: An analysis of variance test for normality (complete samples), Biometrika, 52, 591–611, 1965.

Sheffield, J., Wood, E. F., and Roderick, M. L.: Little change in global drought over the past 60 years, Nature, 491, 435–440, 2012.

Te, N.: Drought Management in the lower Mekong Basin, 3rd Southeast Asia Water Forum, Kuala Lumpur, Malaysia, 2007.

Torrence, C. and Compo, G. P.: A practical guide to wavelet analysis, B. Am. Meteorol. Soc., 79, 61–78, 1998.

Ummenhofer, C. C., D'Arrigo, R. D., Anchukaitis, K. J., Buckley, B. M., and Cook, E. R.: Links between Indo-Pacific climate variability and drought in the Monsoon Asia Drought Atlas, Clim. Dynam., 40, 1319–1334, doi:10.1007/s00382-012-1458-1, 2013.

Wahl, E. R. and Morrill, C.: Toward Understanding and Predicting Monsoon Patterns, Science, 328, 437–438, doi:10.1126/science.1188926, 2010.

Wang, B., Wu, R., and Lau, K. M.: Interannual Variability of the Asian Summer Monsoon: Contrasts between the Indian and the Western North Pacific-East Asian Monsoons, J. Climate, 14, 4073–4090, 2001.

Wang, B., Yang, J., Zhou, T., and Wang, B.: Inter-decadal Changes in the Major Modes of Asian-Australian Monsoon Variability: Strengthening Relationship with ENSO since the Late 1970s*, J. Climate, 21, 1771–1789, 2008.

Ward, P. J., Renssen, H., Aerts, J. C. J. H., van Balen, R. T., and Vandenberghe, J.: Strong increases in flood frequency and discharge of the River Meuse over the late Holocene: impacts of long-term anthropogenic land use change and climate variability, Hydrol. Earth Syst. Sci., 12, 159–175, doi:10.5194/hess-12-159-2008, 2008.

Ward, P. J., Beets, W., Bouwer, L. M., Aerts, J. C. J. H., and Renssen, H.: Sensitivity of river discharge to ENSO, Geophys. Res. Lett., 37, L12402, doi:10.1029/2010GL043215, 2010.

Ward, P. J., Renssen, H., Aerts, J. C. J. H., and Verburg, P. H.: Sensitivity of discharge and flood frequency to 21st Century and late Holocene changes in climate and land use (River Meuse, northwest Europe), Climatic Change, 106, 179–202, 2011.

Wassmann, R., Jagadish, S. V. K., Sumfleth, K., Pathak, H., Howell, G., Ismail, A., Serraj, R., Redona, E., Singh, R. K., and Heuer, S.: Chapter 3 Regional Vulnerability of Climate Change Impacts on Asian Rice Production and Scope for Adaptation, Adv. Agro., 102, 91–133, 2009.

Wolter, K. and Timlin, M. S.: El Niño/Southern Oscillation behaviour since 1871 as diagnosed in an extended multivariate ENSO index (MEI.ext), Int. J. Climatol., 31, 1074–1087, 2011.

Yu, J.-Y., Luand, M.-M., and Seon Tae Kim, S. T.: A change in the relationship between tropical central Pacific SST variability and the extratropical atmosphere around 1990, Environ. Res. Lett., 7, 1–6, 2012.